Research paper

Neighborhood structure influences the convergence in light capture efficiency and carbon gain: an architectural approach for cloud forest shrubs

J. Antonio Guzmán Q.[1,2,3] and Roberto A. Cordero S.[2]

[1]Programa Regional de Posgrado en Biología, Sistema de Estudios de Posgrado, Universidad de Costa Rica, San Pedro 11501, Costa Rica; [2]Laboratorio de Ecología Funcional y Ecosistemas Tropicales, Escuela de Ciencias Biológicas, Universidad Nacional de Costa Rica, Heredia 40101, Costa Rica; [3]Corresponding author (antguz06@gmail.com)

Although plant competition is recognized as a fundamental factor that limits survival and species coexistence, its relative importance on light capture efficiency and carbon gain is not well understood. Here, we propose a new framework to explain the effects of neighborhood structures and light availability on plant attributes and their effect on plant performance in two understory shade-tolerant species (*Palicourea padifolia* (Roem. & Schult.) C.M. Taylor & Lorence and *Psychotria elata* (Swartz)) within two successional stages of a cloud forest in Costa Rica. Features of plant neighborhood physical structure and light availability, estimated by hemispherical photographs, were used to characterize the plant competition. Plant architecture, leaf attributes and gas exchange parameters extracted from the light-response curve were used as functional plant attributes, while an index of light capture efficiency (silhouette to total area ratio, averaged over all viewing angles, STAR) and carbon gain were used as indicators of plant performance. This framework is based in a partial least square Path model, which suggests that changes in plant performance in both species were affected in two ways: (i) increasing size and decreasing distance of neighbors cause changes in plant architecture (higher crown density and greater leaf dispersion), which contribute to lower STAR and subsequently lower carbon gain; and (ii) reductions in light availability caused by the neighbors also decrease plant carbon gain. The effect of neighbors on STAR and carbon gain were similar for the two forests sites, which were at different stages of succession, suggesting that the architectural changes of the two understory species reflect functional convergence in response to plant competition. Because STAR and carbon gain are variables that depend on multiple plant attributes and environmental characteristics, we suggest that changes in these features can be used as a whole-plant response approach to detect environmental filtering in highly diverse tropical forest communities.

Keywords: carbon assimilation, crown architecture, distant-dependence index, plant coexistence, plant interaction.

Introduction

In tropical forest understories, light is one of the most limiting resources (Chazdon and Fetcher 1984, Chazdon and Pearcy 1991). Light availability affects several plant traits and contributes to plant coexistence in different habitats (Hubbell et al. 1999, Adler et al. 2013). Like other resources, light availability varies in a complex way because it changes at different scales, depending on a day and seasonal basis, and on the diffuse effects produced by clouds or vegetation (Craine and Dybzinski 2013). In addition, light resource properties lead to competitive dynamics, where individual investment in plant height improves access to light (Falster and Westoby 2003), while other plants adjust their functional traits to withstand low light regimens (Valladares and Niinemets 2008). In most cases, the interpretation of the effects of competition on plants, specifically light competition, is related to the way in which the competition was measured or defined (Freckleton and Watkinson 1999, Weigelt and Jolliffe 2003). Herein, we use the practical definition of competition described by Grime (1979) and

Trinder et al. (2012) as the capture of essential resources from a common limited pool by neighboring individuals.

In forests where larger individuals decrease the amount of light available to smaller individuals, the process of asymmetric competition occurs (Schwinning and Weiner 1998, Freckleton and Watkinson 1999). In general, four key elements can be identified when plant competition occurs between and within different plant populations: (i) competition zone, e.g., the areas of interaction; (ii) intensity of competition, e.g., the amount of resource captured by neighbors; (iii) competition effect, e.g., the amount of resource available in the neighborhood; and (iv) the responses of the plants to the resource availability (Goldberg 1987, Weigelt and Jolliffe 2003, Berger et al. 2008, Bittebiere et al. 2012). These elements may represent the complexity of plant competition in different neighborhoods, which can be studied using growth features (Trinder et al. 2012) or herein by functional traits and whole-plant performance.

From this standpoint, some researchers have demonstrated correlations between plant functional traits and growth patterns in different gradients of competition (Weiner 1984, Cornwell and Ackerly 2009, Trinder et al. 2013). This suggests that the adaptation to different degrees of competition may allow the coexistence of species and define the assembly of local plant communities. Different plant features have been considered as functional traits that change due to competition, such as specific leaf area (SLA; Butterfield and Callaway 2013), nitrogen content (Trinder et al. 2012), biomass growth (Weiner 1984, Trinder et al. 2013) and height (Falster and Westoby 2003). However, the direct implications of plant competition or neighborhood structure on plant architecture and subsequently on light capture efficiency and carbon gain have seldom been demonstrated. Additionally, which properties of plant competition most influence plant architecture or any other trait has rarely been studied.

It is known that different species with contrasting morphology can converge in their crown architecture to achieve similar light capture efficiency (Valladares et al. 2002, Pearcy et al. 2004), and how these changes are mediated by the shade and sunlight regimens above their crowns (Pearcy et al. 2005, Delagrange et al. 2006). However, does the neighborhood structure have a significant effect on the plant features and consequently on the light capture efficiency and carbon gain more than the light availability alone? Studies have shown that plants under competitive environments adjust their architecture and biomass allocation depending on plant part placement of neighbors in relation to available resources (Tremmel and Bazzaz 1995). For this, we consider that the surrounding structure of the neighborhood around each plant can affect different plant features and their associated performance. This previous affirmation does not discard light availability as a major factor influencing these features. It is expected that plants that can adjust their architectural pattern in contrasting plant neighborhoods or competitive environments may have found a way to survive and coexist in different habitats.

If the above is true, species that can change their functional architecture at different organization levels (e.g., branching, allometry, biomechanics and form) could produce 'optimal' compensatory efficiencies for the particular condition of each local environment, which will allow them to exploit different habitats and survive.

Here, we propose a new framework where we analyze the importance of neighborhood structure on light availability and its implication on plant attributes like gas exchange, plant architecture and leaf attributes (Figure 1). From this, we study how the changes in the plant attributes related to asymmetric competition affect plant performance like light capture efficiency and carbon gain. This was studied in two understory shrub species (*Palicourea padifolia* (Roem. & Schult.) C.M. Taylor & Lorence and *Psychotria elata* (Swartz)) that are found naturally within two cloud forest communities of different successional status in Costa Rica. In general, we address two general hypotheses. (i) Understory plants associate their photosynthetic, leaf attribute and architectural features according to the degree of neighborhood structure. Light availability and the successional status of the cloud forest were established as an ancillary hypothesis to explain plant responses. (ii) Changes in plant architecture, leaf attributes and gas exchange associated with neighborhood structure and consequently with light availability lead to a convergence in the plant performance (light capture efficiency and carbon gain). The purpose of this study is to increase our understanding of how whole-plant responses to asymmetric competition can lead to a convergence of plant functions. Ultimately, this convergence must be considered as a key factor that will contribute to plant community structure in the diverse tropical ecosystems.

Materials and methods

Study site and plant species

We conducted this study at two sites in Río Macho, Cartago, Costa Rica. The first site is a secondary old forest (SOF) of
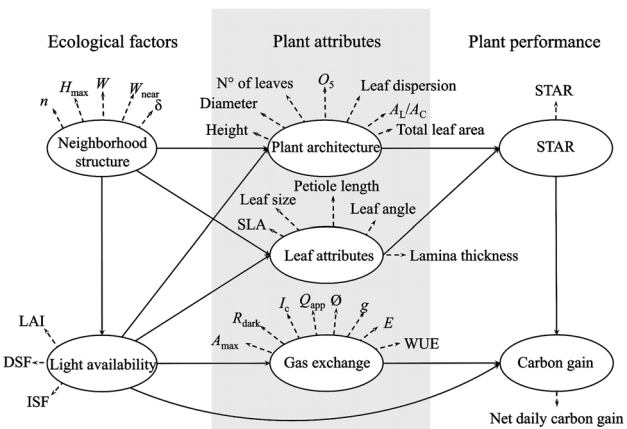
Figure 1. Partial least square Path model, explaining the effect of ecological factors on plant attributes and performance. Solid and dashed lines represent the inner and outer models.

21.26 ha near to Estación de Biología Tropical y Acuicultura (EBTARM) (9°45′52.64″N, 83°51′44.13″W, 1700 m above sea level (a.s.l.)). Annual rainfall is 2416 mm, and the monthly mean temperature is 15.8 °C (Pérez-Molina and Cordero 2012). The most abundant tree species in this site are *Viburnum costaricanum*, *Lozania mutisiana*, *Symphonia globulifera*, *Ilex lamprophylla* and *Dendropanax arboreus*, distributed along three forest canopy strata and topographic slopes between 20 and 50%. The second site is a secondary young forest (SYF) of 11.62 ha to the west of EBTARM (9°45′24.42″N, 83°50′59.16″W, 1700 m a.s.l.). The average rainfall is 2146 mm, and monthly mean temperature is 16.5 °C (Pérez-Molina and Cordero 2012). Some of the most common plant species in this site are *Syzygium jambus*, *Vismia baccifera*, *Miconia dodecandra*, *Myrsine coriacea* and *V. costaricanum*, distributed in at least two forest canopy strata, and topographic slopes lower than 30%. Forest structure and the most common species composition at both sites are presented in Table S1 available as Supplementary Data at *Tree Physiology* Online. According to aerial photographs and interviews, the SOF and SYF forest have 53 and 20 years of natural regeneration, respectively, both from abandoned pastures and soils derived from Ultisol. These sites are classified within the rainy tropical lower montane life zone (ITCR 2008).

Two Rubiaceae plants were used in this study: *P. padifolia* and *P. elata*. *Palicourea padifolia* is a common shrub (2–7 m in height) found in cloud forest from southern Mexico to Panama (Taylor 1989). It can be recognized by reddish-purple pyramidal, terminal inflorescences with yellow, 1-day flowers organized in cymose clusters (Taylor 1989). *Psychotria elata* is an understory shrub (5–8 m in height) of premontane and wet forest from southern Mexico to Ecuador, easy to recognize by inflorescences surrounded by two ovate red involucral bracts. Both species occur in similar light environments in our study area. According to the Hallé et al. (1978) model, both species seem to fit a Koriba architectural model as a result of their sympodial branching, decussated phyllothaxy and branch mortality.

Field design

We choose 10 target plants of *P. padifolia* and *P. elata* at each study site. Each plant was selected by considering plant heights between 1 and 2 m, the absence of obvious mechanical damage or herbivory and growing in sites avoiding strong slopes, and plants that were far from trails. Each plant was separated by more than 5 m between them but including different areas across each site. On these target plants, we measured different features of the neighborhood environment and functional plant traits categorized into seven groups: neighborhood structure, light availability, plant architecture, leaf attributes, gas exchange, light capture efficiency and plant carbon gain. The estimated variables in each group are described below.

Neighborhood structure

All neighboring woody plants (excluding woody climbers and palms) within a 5 m radius that exceed the height at the top of the crown of the target plant were measured. From each neighbor plant, height (h, m), circumference at breast height (c, m), the horizontal orientation with respect to the magnetic north (α) and their distance to the target plant from the stem to stem at 1.3 m (d, m) were measured. The c was measured with a tape (±0.05 cm), α by digital compass (BG, Bushnell, Overland Park, Kansas, USA) and d using a laser range finder (Disto D2, Leica Geosystems AG, Heerbrugg, Switzerland). Tree height (h) was determined by two methods according to the visibility of the tree top crown: direct measurements of the tallest leaf by laser range finder and trigonometry height estimations with a digital clinometer (Forestry Pro, Nikon, Shinagawa-ku, Tokyo, Japan) and laser range finder.

We extracted five characteristics of the neighborhood structure that influence plant features: (i) the number of neighbors (n) or the number of plants falling within the 5 m radius as a density-dependent factor; (ii) maximum neighbor height (H_{max}, m), which relates to the neighborhood size; (iii) tree aggregation index (δ), which is related to the neighbor dispersion; (iv) near tree interference (W_{near}, $m^3\ m^{-1}$), which is related to the nearest interaction factor; and finally, (v) distance-dependent plant interference (W, $m^3\ m^{-1}$), which is related to neighborhood size–distance effect. W was calculated according to the Weiner model (1984), which defines W as:

$$W = \sum_{i=1}^{n} h_i c_i^2 d_i^{-1}, \tag{1}$$

where i is each neighbor plant; n the total number of neighbors; and h, c and d are the height, circumference at breast height and distance as described above. W varies between 0 and ∞, where higher values correspond to higher interference and competition. W_{near} was calculated in the same way except that we used the value of the nearest i neighbor. δ was calculated according to Zar (2010) considering the horizontal orientation of the neighbors as follows:

$$\delta = 1 - \sqrt{\left(\frac{\sum_{i=1}^{n} \sin_{\alpha i}}{n}\right)^2 + \left(\frac{\sum_{i=1}^{n} \cos_{\alpha i}}{n}\right)^2} \tag{2}$$

where i and n are as described above, and α is the horizontal angle of orientation of each neighbor plant. δ varies between 0 and 1, where 0 describes completely aggregated neighborhoods and 1 completely dispersed neighborhoods.

Understory light environment measurement

We measured the light availability of each target plant using hemispherical photographs (Rich 1989) just after harvesting

the plant. The photograph was taken with a digital camera (Sigma EX SD14, Sigma, Setagaya-ku, Japan) equipped with a 35-mm fisheye lens. The camera was leveled at 1.50 m by a tripod and the photo was taken oriented to the magnetic north. Five pictures with different shutter speeds were taken; however, we only selected the picture with the best contrast for the analysis. Resulting images were analyzed with HemiView 2.1 software (Delta-T Instruments, Cambridge, UK). The image processing was performed by creating 160 sky sector (8 azimuth classes and 20 elevation angle classes) and, for a specific day, the time series (1 min interval) of openness along the solar track. From this analyses, direct site factor (DSF), indirect site factor (ISF) and global site factor (GSF) were estimated. Direct site factor and ISF estimate the fraction of direct and diffuse radiation as an index of light availability, respectively, expected to reach the spot where the photo was taken. Global site factor is the mean of DSF and ISF. Additionally, leaf area index (LAI) was estimated as a forest cover indicator above each plant according to the HemiView 2.1 software.

Plant architecture and leaf attributes

We measured for each target plant the individual stem height, the basal diameter at 5 cm aboveground (D_b, cm) and the number of leaves as indicators of the plant architecture. Other parameters described below in the light capture efficiency measurements were also used as proxies of plant architecture, such as crown density, leaf dispersion, distance between leaves and total leaf area. Additionally, we extracted a segment of three mature and fully expanded leaves from the top crown to measure lamina thickness with a digital micrometer (293-349 Mitutoyo, Miyazaki, Japan). These segments were dried at 58 °C for >72 h and weighed to calculate SLA (m^2 kg^{-1}). Other leaf attributes measured were mean petiole length, mean leaf size and mean leaf angle, also described below in the light capture efficiency measurements. All of these parameters are used here as functional features that can change their properties in response to ecological factors (Pérez-Harguindeguy et al. 2013).

Gas exchange analysis

We used a portable photosynthesis system LI-6400 (Li-Cor, Nebraska, USA), open configured, equipped with an artificial light source and carbon dioxide (CO_2) assembly to measure the gas exchange of a mature and fully expanded leaf from the top crown of each plant. We obtained light and CO_2 response curves following Tambussi and Graciano (2010). Leaf temperature was maintained between 25 and 27 °C, and relative humidity was kept between 65 and 80% for both protocols. Light-response curves ($A–I$) were obtained using a CO_2 concentration of 390 p.p.m. According to previous light-response data, carbon assimilation was measured at irradiances ranging from 1500 to 0 μmol m^{-2} s^{-1} with leaves pre-illuminated at 1000 μmol m^{-2} s^{-1} for 5–7 min. Carbon assimilation (A) versus irradiance (I) was

fitted using a nonrectangular hyperbola model (Marshall and Biscoe 1980, Thornley and Johnson 1990) to extract the following leaf photosynthetic parameters: maximum assimilation rate (A_{max}, μmol CO_2 m^{-2} s^{-1}), dark respiration rate (R_{dark}, μmol CO_2 m^{-2} s^{-1}), apparent quantum yield (Q_{app}, μmol CO_2 m^{-2} s^{-1}/ μmol m^{-2} s^{-1}) and the curvature of the regression (θ). Light compensation point (I_c, μmol m^{-2} s^{-1}) was calculated independently by 'x' line interception of linear regression analysis of data points between 0 and 60 μmol m^{-2} s^{-1} of light. This model was fit by the $nls2$ package (Grothendieck 2014) of R software (R Development Core Team 2014). We extracted from irradiances of 1000 μmol m^{-2} s^{-1} the leaf conductance (g, mmol H_2O m^{-2} s^{-1}), transpiration (E, mmol H_2O m^{-2} s^{-1}) and CO_2 assimilation (A_{1000}), and then we calculated the water use efficiency (WUE, μmol CO_2 m^{-2} s^{-1}/mmol H_2O m^{-2} s^{-1}) by the ratio of A_{1000}/E.

We carried out the CO_2 response curve ($A–C_i$) after the light-response curve in the same leaf, varying the CO_2 concentration between 50 and 900 p.p.m. at light irradiance of 1000 μmol m^{-2} s^{-1} and atmospheric pressure of 86–87 Pa. Carbon dioxide assimilation versus internal carbon concentration (C_i) data were fitted following the Ethier and Livingston (2004) version of Farquhar's model (Farquhar et al. 1980) to extract the following leaf biochemical parameters: maximum rate of carboxylation (V_{cmax}, μmol CO_2 m^{-2} s^{-1}), maximum photosynthetic electron flow rate (J_{max}, μmol e^- m^{-2} s^{-1}), day respiration rate (R_{day}, μmol CO_2 m^{-2} s^{-1}), chloroplast CO_2 compensation point (Γ, μmol mol^{-1}) and mesophyll conductance (g_i, mmol CO_2 m^{-2} s^{-1}). All of these parameters extracted from $A–I$ and $A–C_i$ curves were used to quantify the photosynthetic capacity and as a possible indicator of physiological acclimation (Pearcy 1987).

Crown architecture

We measured the crown architecture according to Pearcy and Yang (1996) following the protocol of Pearcy et al. (2013) in order to calculate light capture efficiency and whole-plant carbon gain according to Duursma et al. (2012) and Pearcy and Yang (1996), respectively. These methodologies consider the node as the basic form, where the articulated sum of nodes, petioles and leaves with their orientations, distributions and size reflects the three-dimensional plant architecture (Pearcy and Yang 1996). For this, each node, petiole and leaf blade were described by its length and diameter (except leaf blade) with digital calipers (±0.005 mm), orientation according to the true north with a digital compass (±1 °) and inclination from the horizontal with a digital clinometer (±0.05 °); however, in the leaf blade, the orientation and leaf angle (inclination) were considered from the vector of the steepest angle of the leaf surface. For each species, the leaf shape was standardized by establishing 38 point marks along the leaf silhouette using an x, y coordinate system centered in the leaf blade base. Schematic description of a plant in the field and its three-dimensional plant

and crown architecture are shown in Figure S1 available as Supplementary Data at *Tree Physiology* Online.

Light capture efficiency

After obtaining the three-dimensional plant architecture for each individual, we measured the light capture efficiency by an index of the silhouette to total area ratio, averaged over all viewing angles (STAR, $m^2 \, m^{-2}$) calculated by YplantQMC R package (Duursma and Cieslak 2013) according to Duursma et al. (2012). This index was obtained with a grid-tracer leaf area method of a size 100 grid and 244 sectors placed uniformly over the hemisphere. This method determines at each sector on the hemisphere the ratio of the silhouette or displayed area (A_D, m^2) from the intersecting grid points to the estimated total leaf area (A_L, m^2), to then extract the average of A_D/A_L across all sectors over the hemisphere. STAR, averaged over all viewing angles, values produced ranges of 0–0.5, where 0.5 describe a plant without overlapped leaves and, therefore, with a greater light interception efficiency.

Likewise, other parameters indicative of plant architecture were extracted by YplantQMC like the number of leaves, the leaf dispersion (the ratio of observed average distance to five nearest leaves between the expected average distances to five nearest leaves for a random distribution), the observed average distance to five nearest leaves (O_5, m), the crown density (A_L/A_C, the ratio of A_L to the total surface area of 3D convex hull wrapped around the leaf cloud) and A_L. Parameter proxies of leaf attributes, such as the mean leaf size, mean leaf angle and mean petiole length, were also extracted from all plant leaves.

Simulation of whole-plant carbon gain

We used the gas exchange parameters extracted by the light curve response, the crown architecture, the understory light environment and atmospheric characteristics of each target plant to simulate the whole-plant carbon gain by YPLANT 3.2 (Pearcy and Yang 1996). From this, leaf photosynthetic parameters such as A_{max}, R_{dark}, Q_{app} and θ were extracted from previous analyses of gas exchange. Constant values of 0.85 and 0.05 for leaf absorbance and transmittance, respectively, were used according to Pearcy et al. (2013). HemiView output as gap fractions of the 160 sky sectors and the fraction of the solar disk visible through the gap in 21 March (spring equinox) were used as characteristics of understory light regimes. Minimum and maximum temperatures of 12.5 and 23.5 °C, respectively, 390 p.p.m. of CO_2 atmospheric concentrations and 82 Pa of air pressure were used as the input values for atmospheric characteristics. Twenty-four hours of carbon gain (net carbon gain) for the leaves of each target plant was estimated at the spring equinox (21 March), when there is 12 h of daylight at the latitude of 9.76N. Because YPLANT 3.2 estimates only the net daytime assimilation per unit leaf, 12 h of darkness carbon balance (respiration) was subtracted by the dark respiration per foliage per minute, similar to Lusk et al. (2011).

Statistical analyses

We compared the light environment and neighborhood characteristics across sites for each species using a multivariate analysis of variance (MANOVA). Then we extracted the univariate analysis of variance (ANOVA) to interpret the overall multivariate effects on each variable. For each species, we compared the plants' architecture and leaf attributes, light curve response parameters and CO_2 curve response parameters across sites using MANOVA and extracted the univariate ANOVA in each comparison. In all MANOVA, we extracted the Hotelling–Lawley statistic to describe the multivariate effect according to Quinn and Keough (2002). Within each species, we used a *t*-test to compare the effect of the sites on STAR and net carbon gain. We also applied two analyses of covariance (ANCOVAs) within each species to measure the effect of A_L/A_C and leaf dispersion as covariate factor on STAR, and using the site as a categorical factor. We conducted the previous analyses using R software version 3.1.1 (R Development Core Team 2014).

We employed a partial least square (PLS) Path model for each plant species to measure how the neighborhood structure can affect the light availability, and how these ecological factors can affect the plant architecture, leaf attributes and gas exchange and their implication for STAR and net carbon gain (Figure 1). We conducted this analysis due to the soft assumptions of normal distribution, sample size and multicollinearity of the field data. We used SmartPLS 3.1 software (Ringle et al. 2014) to conduct this analysis, where we implemented a path weighting scheme to estimate the inner values of the standardized latent variable and a bootstrapping of 5000 iterations based on the individual changes to extract the variation of the inner and outer variables and their significance according to two-tailed *t*-tests.

Results

Neighborhood and light availability

The neighborhood structure and light availability around of each species were different between SOF and SYF (*P. padifolia*: Hotelling–Lawley$_{(9,10)}$ = 6.94, $P < 0.01$; *P. elata*: Hotelling–Lawley$_{(9,10)}$ = 14.69, $P < 0.001$) (Table 1). In the surrounding neighborhood of *P. padifolia*, differences in parameters of the physical structure between sites were found in n and W, where plants in the SOF showed higher values of W and a lower amount of neighbors than plants in the SYF. In *P. elata*, differences in parameters of the surrounding physical structure were found only in H_{max}, where neighbors in the SOF showed higher values than neighbors in the SYF. Neighborhood characteristics like W_{near} and δ did not differ between sites within each species. The light features of the surrounding neighborhood of each species showed higher values of light availability (DSF, ISF and GSF) and

LAI in SYF than SOF. These results confirm that both species overlap their light regimes within each site (Table 1).

Plant architecture and leaf attributes

The responses of the architecture and leaf attributes within each species across sites showed differences in *P. eltata* (Hotelling–Lawley$_{(12,7)}$ = 7.35, P = 0.04) but not in *P. padifolia* (Hotelling–Lawley$_{(12,7)}$ = 3.72, P = 0.16). The univariate response in *P. elata* suggests that differences were found in D_b, mean leaf size, O_5, SLA and leaf thickness, where plants in the SYF present higher value of D_b and lower values of mean leaf size, O_5, SLA and leaf thickness than plants in the SOF (Table 2). Although *P. padifolia* did not show a multivariate response across sites, the univariate analyses suggest that plants of *P. padifolia* in the SYF present high value of D_b and lower values of mean petiole length and SLA than plants in the SOF.

Gas exchange

The multivariate comparison within each species across sites on the parameters extracted from the light curve and CO_2 curve

Table 1. Neighborhood structure and light availability estimated by interference measures and hemispherical canopy photography of *P. padifolia* and *P. elata* in two cloud forests of different successional status, Río Macho, Costa Rica: SYF and SOF. Values are the mean (n = 20) and the standard deviation. Significant differences between sites are represented by a posteriori ANOVA test extracted from MANOVA. n, number of neighbors; H_{max}, maximum neighbor height; W_{near}, near tree interference; W, distance-dependent plant interference; δ, tree aggregation index; LAI, leaf area index; DSF, direct site factor; ISF, indirect site factor; GSF, global site factor. P-values for each ANOVA are given next to the F values (*P, 0.05; **P, 0.01; ***P, 0.001).

Characteristics	Species					
	Palicourea padifolia			Psychotria elata		
	SYF	SOF	F	SYF	SOF	F
Neighborhood features						
n	47.70 ± 14.41	29.00 ± 9.41	10.13**	41.80 ± 9.83	38.50 ± 9.07	0.58
H_{max} (m)	15.05 ± 2.68	16.22 ± 3.65	0.53	14.57 ± 2.28	17.36 ± 3.10	5.03*
W_{near} (m^3 m^{-1})	1.04 ± 1.59	1.60 ± 3.48	0.05	1.06 ± 1.62	1.74 ± 3.24	3.97
W (m^3 m^{-1})	18.70 ± 5.13	28.45 ± 11.52	4.76*	28.39 ± 16.25	28.11 ± 12.27	0.07
δ	0.85 ± 0.07	0.77 ± 0.07	2.18	0.86 ± 0.09	0.84 ± 0.14	0.23
Light characteristics						
LAI	2.10 ± 0.29	3.10 ± 0.60	23.63***	2.13 ± 0.30	3.07 ± 0.65	22.10***
DSF	0.19 ± 0.05	0.16 ± 0.03	2.25	0.22 ± 0.07	0.14 ± 0.03	10.17**
ISF	0.17 ± 0.04	0.12 ± 0.02	12.45**	0.18 ± 0.05	0.12 ± 0.02	19.87***
GSF	0.19 ± 0.05	0.15 ± 0.03	2.65	0.21 ± 0.07	0.14 ± 0.03	11.13**

Table 2. Plant architecture and leaf traits of *P. padifolia* and *P. elata* in two cloud forests of different successional status, Río Macho, Costa Rica: SYF and SOF. The values are the mean (n = 10) and the standard deviation per species at each site. Significant differences between sites across species and significant differences between species, site and its interaction are represented by a posteriori ANOVA text extracted from MANOVA. D_b, basal diameter; O_5, the observed average distance to five nearest leaves; A_L/A_C, crown density (the ratio of A_L to the total surface area of 3D convex hull wrapped around the leaf cloud); SLA, specific leaf area. P-values for each ANOVA are given next to the F values (*P, 0.05; **P, 0.01; ***P, 0.001).

Parameters	Species					
	Palicourea padifolia			Psychotria elata		
	SYF	SOF	F	SYF	SOF	F
Plant architecture						
Height (m)	1.73 ± 0.22	1.67 ± 0.23	0.22	1.52 ± 0.23	1.50 ± 0.21	0.03
D_b (cm)	1.32 ± 0.25	1.08 ± 0.18	6.32*	1.32 ± 0.23	1.04 ± 0.20	8.26*
Number of leaves	62.50 ± 25.43	59.30 ± 23.21	0.17	80.70 ± 34.58	58.10 ± 24.09	2.08
O_5 (m)	0.09 ± 0.01	0.10 ± 0.01	2.91	0.09 ± 0.01	0.11 ± 0.01	16.31***
Leaf dispersion	0.93 ± 0.08	0.93 ± 0.09	0.01	0.89 ± 0.07	0.95 ± 0.09	2.58
A_L/A_C	0.18 ± 0.03	0.16 ± 0.03	2.09	0.23 ± 0.06	0.21 ± 0.05	1.02
Total leaf area (m^2)	0.21 ± 0.10	0.22 ± 0.10	0.20	0.31 ± 0.16	0.29 ± 0.08	0.01
Leaf traits						
Mean leaf size (cm^2)	32.59 ± 3.08	38.56 ± 10.32	1.82	38.46 ± 6.56	51.50 ± 10.19	12.16**
Mean leaf angle (°)	31.04 ± 9.55	30.98 ± 5.18	0.02	22.84 ± 8.56	27.96 ± 6.60	2.80
Mean petiole length (mm)	8.39 ± 2.00	11.10 ± 4.36	5.60*	9.95 ± 2.45	17.92 ± 5.09	18.64***
SLA (m^2 kg^{-1})	19.78 ± 4.40	24.06 ± 3.45	6.87*	19.29 ± 2.01	25.22 ± 2.09	40.99***
Lamina thickness (mm)	0.19 ± 0.02	0.18 ± 0.02	2.26	0.24 ± 0.07	0.19 ± 0.05	6.96*

Table 3. Gas exchange parameters extracted from light and CO_2 curve responses of *P. padifolia* and *P. elata* in two cloud forests of different successional status, Río Macho, Costa Rica: SYF and SOF. Values are the mean ($n = 10$) and the standard deviation. Significant differences between sites across species are represented by a posteriori ANOVA text extracted from MANOVA. A_{max}, maximum assimilation rate; R_{dark}, dark respiration rate; I_c, light compensation point; Q_{app}, apparent quantum yield; θ, curvature; g, leaf conductance; E, transpiration; WUE, water use efficiency; V_{cmax}, maximum rate of carboxylation; J_{max}, maximum photosynthetic electron flow rate; R_{day}, day respiration rate; Γ, chloroplast CO_2 compensation point; g_i, mesophyll conductance. *P*-values for each ANOVA are given next to the *F* values (*P, 0.05).

Parameters	Species					
	Palicourea padifolia			*Psychotria elata*		
	SYF	SOF	*F*	SYF	SOF	*F*
Light curve response						
A_{max} (μmol CO_2 m^{-2} s^{-1})	5.38 ± 0.56	4.97 ± 0.83	1.83	4.35 ± 0.74	4.16 ± 0.62	0.33
R_{dark} (μmol CO_2 m^{-2} s^{-1})	0.23 ± 0.11	0.30 ± 0.21	0.21	0.22 ± 0.10	0.13 ± 0.06	5.76*
I_c (μmol m^{-2} s^{-1})	2.72 ± 1.28	3.38 ± 2.41	0.19	2.54 ± 1.31	1.54 ± 0.71	4.91*
Q_{app} (μmol CO_2 m^{-2} s^{-1}/μmol m^{-2} s^{-1})	0.09 ± 0.03	0.09 ± 0.01	0.01	0.09 ± 0.01	0.09 ± 0.02	1.18
θ (–)	0.17 ± 0.22	0.16 ± 0.26	0.09	0.09 ± 0.14	0.17 ± 0.21	0.76
g (mmol H$_2$O m^{-2} s^{-1})	0.09 ± 0.03	0.08 ± 0.04	0.23	0.06 ± 0.02	0.05 ± 0.03	2.19
E (mmol H$_2$O m^{-2} s^{-1})	1.03 ± 0.29	0.91 ± 0.35	0.74	0.86 ± 0.25	0.61 ± 0.31	4.40
WUE (μmol CO_2 m^{-2} s^{-1}/mmol H$_2$O m^{-2} s^{-1})	5.08 ± 1.34	5.51 ± 2.26	0.15	4.82 ± 1.01	8.21 ± 3.82	1.20
CO_2 curve response						
V_{cmax} (μmol CO_2 m^{-2} s^{-1})	15.75 ± 3.25	15.09 ± 4.00	0.27	14.21 ± 4.20	13.95 ± 4.33	0.07
J_{max} (μmol e$^-$ m^{-2} s^{-1})	40.12 ± 8.99	43.40 ± 10.79	0.51	38.77 ± 5.71	37.06 ± 8.93	0.39
R_{day} (μmol CO_2 m^{-2} s^{-1})	0.30 ± 0.15	0.20 ± 0.09	4.85*	0.28 ± 0.11	0.25 ± 0.09	0.61
Γ (μmol mol^{-1})	5.52 ± 0.65	4.97 ± 0.38	6.21*	5.29 ± 0.36	5.40 ± 0.33	0.47
g_i (mmol CO_2 m^{-2} s^{-1})	165.42 ± 1.86	154.95 ± 3.15	0.61	154.52 ± 1.85	130.16 ± 2.69	5.70*

responses showed that the gas exchange traits differed between sites in *P. elata* (Hotelling–Lawley$_{(13,6)}$ = 14.22, $P = 0.04$) but not in *P. padifolia* (Hotelling–Lawley$_{(13,6)}$ = 6.23, $P = 0.19$). The univariate responses in *P. elata* suggest that differences were found in R_{dark}, I_c and g_i, where plants in the SYF present higher values of these parameters than plants in the SOF (Table 3). Although *P. padifolia* did not show differences in the multivariate response of gas exchanges across sites, the univariate analyses suggest that plants in the SYF present higher values of R_{day} and Γ than plants in the SOF.

Plant performance

Comparisons between sites of the modeled plants within species showed that plants did not differ either in STAR (*P. pafifolia*: $t_{19} = -1.70$, $P = 0.11$; *P. elata*: $t_{19} = -1.71$, $P = 0.11$, Figure 2a) or in net daily carbon gain (*P. pafifolia*: $t_{19} = 1.07$, $P = 0.30$; *P. elata*: $t_{19} = 0.06$, $P = 0.95$, Figure 2b). In both species, the STAR responds significantly to A_L/A_C (see Table S2 available as Supplementary Data at *Tree Physiology* Online) but not to leaf dispersion, sites or their interactions (A_L/A_C sites and leaf dispersion sites). In both species across sites, increases in A_L/A_C led to decreases in STAR (Figure 3a and c).

Partial least square Path model

Our framework showed that the ecological factors have important effects on several plant attributes and their performance (Figure 4). This was expressed significantly by two pathways in
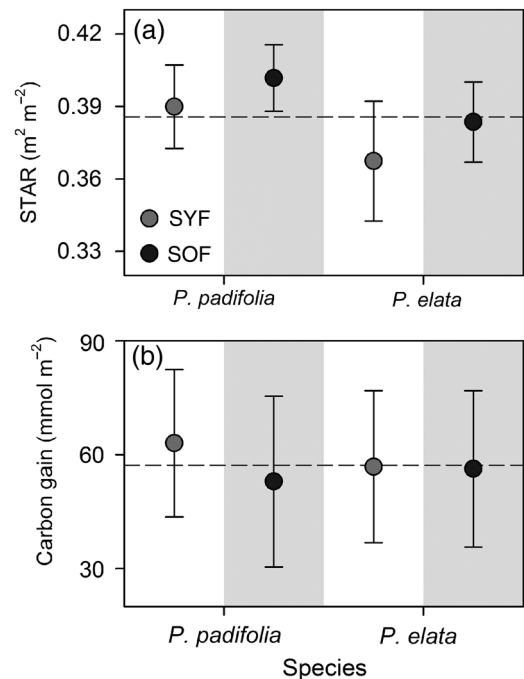

Figure 2. STAR, averaged over all viewing angles, and net daily carbon gain of *P. padifolia* and *P. elata* in two cloud forests of different successional status, Río Macho, Costa Rica: SYF and SOF. Circles are the mean ($n = 10$), errors bars the standard deviation and dashed lines represent the population mean.

both species. First, neighborhood structure influences plant architecture, and this architecture affects STAR and consequently carbon gain. Second, neighborhood structure mostly
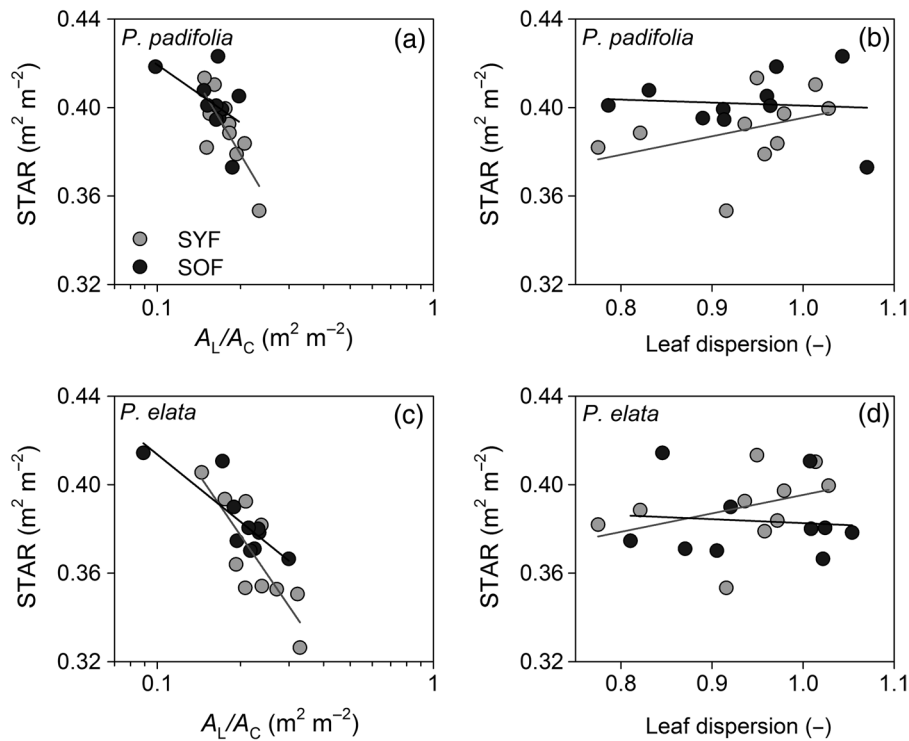
Figure 3. STAR, averaged over all viewing angles, related to crown density (the ratio of leaf area (A_L) to crown surface area (A_C)) and leaf dispersion of *P. padifolia* and *P. elata* in two cloud forests of different successional status, Río Macho, Costa Rica: SYF and SOF. One-way ANCOVA results are represented in Table S2 available as Supplementary Data at *Tree Physiology* Online.
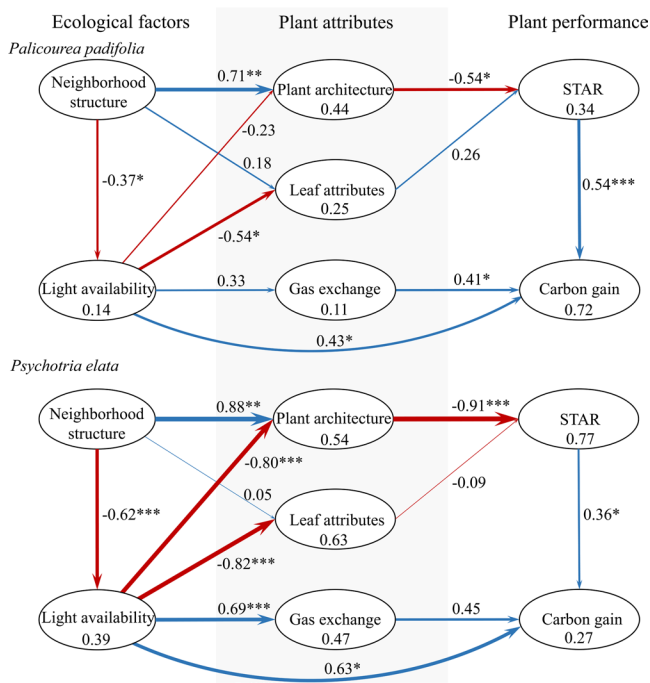

Figure 4. Partial least square Path model results explaining the effect of ecological factors on plant attributes and performance. Path coefficients and their significance, extracted by bootstrapping, are given near the arrows, values within ellipses are the proportions of variance explained by the model. Outer loadings are presented in Table 4. *P, 0.05; **P, 0.01; ***P, 0.001.

modifies light availability and the resulting light regime influences carbon gain (Figure 4; see Table S3 available as Supplementary Data at *Tree Physiology* Online). Although light availability in both species was associated with changes in leaf attributes, these features showed no influence on plant performance. In *P. elata*, light availability was related to changes in gas exchange, but only in *P. padifolia* was gas exchange related to carbon gain. In general, the neighborhood structure explained 14 and 39% of light availability in *P. padifolia* and *P. elata*, respectively. This structure of neighbors was explained mainly by W and δ in *P. padifolia* and W and H_{max} in *P. elata* (Table 4), where increases in the structure produce decreases in light availability and changes in plant architecture traits. Together, neighborhood structure and light availability explained 44 and 54% of plant architecture variance, and 25 and 63% of the variance on leaf attributes in *P. padifolia* and *P. elata*, respectively. All light availability variables (ISF, DSF and LAI) showed significant weight on their latent group. In both species, the A_L, number of leaves, A_L/A_C and O_5 were shown to be variables that have significant influence on plant architecture, while only SLA, leaf thickness and petiole length were variables that influence the leaf attributes group. In *P. padifolia* and *P. elata*, plant architecture and leaf attributes explained 28 and 77% of the STAR variance, respectively, but only the plant architecture group had a significant effect. In general, changes in plant architecture promote increases in STAR. Light availability, gas exchange

Table 4. Loadings of the outer model and bootstrapping results (mean ± standard error (SE), and *t*-test) from the PLS Path model, explaining the effect of ecological factors on plant attributes and performance. The inner variables are presented in bold. W, distance-dependent plant interference; n, number of neighbors; δ, tree aggregation index; H_{max}, maximum neighbor height; W_{near}, near tree interference; DSF, direct site factor; ISF, indirect site factor; LAI, leaf area index; A_L/A_C, crown density; O_5, the observed average distance to five nearest leaves; SLA, specific leaf area; A_{max}, maximum assimilation rate; E, leaf transpiration; I_c, light compensation point; Q_{app}, apparent quantum yield; R_{dark}, dark respiration rate; WUE, water use efficiency; g, leaf conductance; θ, curvature; STAR, silhouette to total area ratio, averaged over all viewing angles, the light capture efficiency. *P*-values for each bootstrapping are given next to the *t*-test (*P, 0.05; **P, 0.01; ***P, 0.001).

Outer model	Species					
	Palicourea padifolia			*Psychotria elata*		
	Loadings	Mean ± SE	*t*-Test	Loadings	Mean ± SE	*t*-Test
Neighborhood structure						
W	0.81	0.72 ± 0.19	4.16***	0.81	0.75 ± 0.19	2.12***
n	0.41	0.53 ± 0.29	1.44	0.43	0.52 ± 0.25	1.75
δ	−0.76	−0.59 ± 0.26	2.89**	−0.10	−0.37 ± 0.21	0.45
H_{max}	−0.04	−0.03 ± 0.23	0.16	0.83	0.61 ± 0.27	3.10**
W_{near}	−0.28	−0.40 ± 0.24	1.14	−0.13	−0.49 ± 0.30	0.44
Light availability						
DSF	0.90	0.86 ± 0.11	8.28***	0.96	0.96 ± 0.02	42.64***
ISF	0.97	0.95 ± 0.08	12.03***	0.98	0.97 ± 0.02	45.18***
LAI	−0.73	−0.76 ± 0.14	5.12***	−0.60	−0.58 ± 0.19	3.01**
Plant architecture						
A_L/A_C	0.71	0.61 ± 0.25	2.87**	0.77	0.68 ± 0.22	3.52***
Basal diameter	−0.12	−0.45 ± 0.24	0.50	0.34	0.48 ± 0.23	1.48
Plant height	0.32	0.36 ± 0.21	1.51	0.05	0.45 ± 0.26	0.18
Leaf dispersion	0.49	0.58 ± 0.26	1.9	−0.23	−0.47 ± 0.27	0.85
No. of leaves	0.65	0.66 ± 0.27	2.37*	0.67	0.66 ± 0.26	2.59**
O_5	0.64	0.52 ± 0.26	2.49*	0.76	0.70 ± 0.20	3.85***
Total leaf area	0.73	0.69 ± 0.20	3.52***	0.54	0.55 ± 0.24	2.01*
Leaf traits						
Leaf thickness	−0.82	−0.69 ± 0.22	3.80***	−0.80	−0.77 ± 0.12	6.44***
Mean leaf angle	0.64	0.52 ± 0.25	2.51*	0.44	0.49 ± 0.23	1.90
Mean leaf size	0.43	0.57 ± 0.24	1.77	0.79	0.79 ± 0.10	7.68***
Petiole length	0.46	0.59 ± 0.26	2.49*	0.87	0.87 ± 0.05	17.72***
SLA	0.94	0.80 ± 0.22	4.26***	0.83	0.81 ± 0.11	7.45***
Gas exchange						
A_{max}	0.71	0.66 ± 0.23	3.15**	0.64	0.59 ± 0.23	2.61**
E	0.92	0.85 ± 0.16	5.97***	0.81	0.70 ± 0.25	3.19***
I_c	0.10	0.38 ± 0.24	0.43	0.88	0.84 ± 0.14	6.13***
Q_{app}	0.45	0.45 ± 0.21	2.15*	−0.09	−0.28 ± 0.21	0.42
R_{dark}	0.16	0.39 ± 0.25	0.65	0.83	0.81 ± 0.15	5.62***
WUE	−0.84	−0.74 ± 0.20	4.28***	−0.69	−0.62 ± 0.24	2.84**
g	0.87	0.79 ± 0.18	4.74***	0.76	0.66 ± 0.24	3.16**
θ	−0.46	−0.44 ± 0.24	1.83	−0.35	−0.36 ± 0.20	1.77
STAR						
STAR	1	–	–	1	–	–
Carbon gain						
Carbon gain	1	–	–	1	–	–

and STAR explained 70 and 27% of net daily carbon gain in *P. padifolia* and *P. elata*, respectively, but only the increases in light availability and STAR had a significant effect on the increases in carbon gain. In both species, A_{max}, E, g and WUE were outer factors associated with changes in gas exchange. However, in *P. padifolia*, these changes were associated also with Q_{app}, while in *P. elata*, gas exchange variations were associated with I_c and R_{dark}.

Discussion

Ecological factors

This study is a first approximation disentangling the relative impact of the neighborhood structure on plant features and their performance. In addition, this study shows the direct effect of the neighborhood structure on some plant features more than the light availability, which highlights the importance of surrounding

neighborhood on plan performance. Specifically, the results indicate that the species studied are experiencing particular habitats with contrasting neighborhood structure and light availability. Following this, the highest amount of n are indicative of early successional stages (Finegan 1996), and the highest H_{max} is a typical feature of late successional stages (Huston and Smith 1987). The similarity in neighborhood aggregation and W_{near} between sites suggests that the directionality and distance of interaction are homogeneously distributed around each plant. Although W was a variable that had greater weight in the neighborhood structure according to the PLS model in both species, this was only different in the surrounding neighborhood of *P. padifolia*. In general, the differences in number and size of neighbors around each plant can explain the interference values, where the value of W in SYF is explained by the number of neighbors and in the SOF by the neighbors' size. The resulting light availability from distance-dependent interference can affect the plant attributes and their performance according to the neighborhood structure between sites, and also depends on particular properties of the neighborhood structure within each site. These effects could have implications on the quality of light for these and other species in the understory, because the quality of light in the understory depends on the stage of succession of the forest and their species composition (Kabakoff and Chazdon 1996, Kitajima et al. 2005), although this latter aspect was not addressed in this study.

The light patterns showed that the SOF understory presents dimmer light regimes than the SYF understory, probably due to neighbor sizes and leaf cover above each plant. However, both species overlapped in their light environments within each forest. According to the PLS Path model, this light availability responds concomitantly to the surrounding neighborhood, specifically through distance-dependence features. This is consistent with studies that suggest that neighborhood indices based on the relative effects of the size and distance of neighboring trees could be used to determine canopy light index (Grote et al. 2013). Moreover, the path coefficients of the light environment variables (ISF, DSF and LAI) resulted in an ecological factor with great weight on leaf attributes and carbon gain. Like other studies, light availability has a strong influence on leaf attributes like SLA, petiole length, leaf size and carbon gain (Valladares et al. 2002).

Plant architecture and leaf attributes

Plant architecture and leaf trait responses could be separated in to three groups: attributes affected by the species, by the site and the attributes not affected by either of these. It is clear that in many cases, the response of attributes may have overlapping effects between the first two groups, because the intrinsic responses of any plant's traits, especially shade-tolerant species, depend on the genetics and ecological features of each plant with their environment (Valladares and Niinemets 2008).

Previous analyses had shown that the patterns of crown density, leaf angle and total leaf area responded at the species level (Guzmán 2015), while D_b, mean petiole length, O_5 and SLA are variables that changed according to the site features. In many cases, increases in the distance between leaves or the petiole length and decreases in the SLA have been described as a strategy to increase the light capture in dimmer light environments, allowing decreases in leaf overlapping (Gálvez and Pearcy 2003) and increases the amount of light that can be intercepted per unit leaf dry mass (Evans and Poorter 2001), respectively.

Whatever the effect on attributes, changes between sites within species have been developed as strategies for increasing the plant performance, which allow them to survive and coexist within communities (Reich et al. 2003, Adler et al. 2013). For example, increases in SLA in the SYF could be associated with a resource-acquisitive leaf economics strategy typical of high-light gap environments, while decreases in the SLA in SOF could be associated with a resource-conservative strategy typical of dimmer light regimens (Adler et al. 2013). Thus, the resulting variations of these strategies in a competitive scenario could prevent the environmental filtering of the species, and may promote plant coexistence in the communities.

Gas exchange

Gas exchange traits did not show a differential responses between sites in *P. padifolia* and show a slight difference in *P. elata*, which suggests a similitude of photosynthetic performance of each species regardless of the state of forest succession (Allen and Pearcy 2000). This latter could be related to a general response of photosynthesis of shade-tolerant species to light environments, where in many cases, these species are described as plants with little phenotypic plasticity at the level of leaf physiology (Valladares and Niinemets 2008). In terms of their responses, Medrano et al. (2002) suggest that the resistance in the transport of molecules (CO_2 and H_2O) inside and outside of leaf mesophyll can limit different physiological processes. It is possible that the absence of conductance effects like g_i (except in *P. elata*) or g was responsible for the absence of variations in A_{max}, WUE, V_{cmax} and J_{max} between sites. Changes in WUE have been observed in other studies adducing strong effects on transpiration due to greater radiation load between sites (Kuiper 1961); however, here, this pattern was not observed. Although there are multivariate differences of gas exchange within sites in *P. elata*, the similarities of V_{cmax} and J_{max} in both species across sites suggest that the biochemical ability of carboxylation and electron flow in the leaves do not exhibit symptoms of photosynthetic stress. In many cases, differences in the carboxylation and electron flow in leaves are the result of environmental stress like high radiation or high temperature and they will have strong implications in other processes like assimilation, respiration or the light compensation point (Niinemets et al. 1998). Then, results such as differences in R_{dark} and I_c in

P. elata are the product of the leaf physiological adaptation to each site rather than the stress effect of each environment.

Contrary to previous interspecific studies in *Psychotria* species with light-demanding and shade-tolerant plants (Pearcy et al. 2004), the gas exchange parameters here had a slight or no effect on carbon gain. However, this result is probably due to the low range of variations in gas exchange values and the low plasticity in the leaf physiology presented by shade-tolerant plants in comparison with light-demanding species (Valladares and Niinemets 2008).

Plant performance

These plants exhibit different changes in the functional traits, but not all changes can increase or affect the plant performance. In this study, the results suggest that STAR performance is mainly affected by A_L/A_C, A_L, O_5 and number of leaves, suggesting an important role of plant architecture. These features along with some other leaf attributes explained more than of 28 and 77% of STAR performance in *P. padifolia* and *P. elata*, respectively. This is consistent with Duursma et al. (2012), who suggest that >42% of STAR is explained by A_L/A_C, and highlighted the great role of leaf dispersion, number of leaves and total leaf area in the light capture function. Although in this study the leaf attributes had minor effects on STAR, other authors showed how changes in the petiole length and leaf size may affect the light capture due to the implications for leaf distribution and self-shading (Takenaka 1994, Gálvez and Pearcy 2003). In this sense, architectural traits have greater effect on plant performance than leaf attributes, which suggests that the crown traits override the individual leaf response in a way that changes in A_L/A_C can promote a convergence response on STAR in both species. However, which of these plant attributes can have a greater impact on STAR performance due to asymmetric competition? Although there are some traits highly correlated with STAR, in a natural environment with an asymmetric competition, the multidimensional response of the plant attributes can affect STAR performance more than a single variable per se. From this perspective, trade-off analysis has shown that individual plant attributes respond in different ways from each other (Wright et al. 2005, Shipley et al. 2006). This situation provides a plethora of compensating effects for the survival in different environments or asymmetric interactions for plants in natural environments.

Regardless of the light environment, plants of both species at both sites present a convergence in the net daily carbon gain. Previous studies point out that changes in light environment, STAR and gas exchange have strong implications on carbon gain (Pearcy 1987, Evans and Poorter 2001). However, our results suggest that some plant attributes have a great capacity for adjustment due to the neighborhood competition and that the smaller changes in gas exchange along with the corresponding architectural adjustments between sites can cause a compensatory effect on net daily carbon gain. This later point could have

significant ecological consequences for these understory species, as discussed below.

Implications of neighborhood structure on plant performance

Even though our sample size is slightly small, our results are in agreement with the general trend reported in the literature and they show a novel way to explain the effects of plant competition on plant performance. It is possible that the compensatory effect of the neighborhood structure on light capture efficiency and whole-plant carbon gain could play an important role in the coexistence of these species at this cloud forest. The compensatory effects of plant attributes may allow an 'optimal' plant performance according to the neighborhood competition in a way that survival could be maximized in different environments. This suggests that the convergence in plant functions with respect to light capture efficiency and carbon gain may subtly prevent niche partitioning for the light resource through site-specific adaptation of plant traits. Thus, it is likely that the functional convergence of plant traits may explain the presence of these shade-tolerant species both in the old and young successional stages. Similar conclusions may be found in the Sterck et al. (2013) experiments based on the light compensation point of the plant, where they suggest that the plasticity in the plant physiology of shade-tolerant and -intolerant tropical understory species is a specialization to neutralize the separation of light niches among species. The point of view of Sterck et al. (2013) and our results suggest that the similarities of the individual fitness obtained by plasticity or local adaptation could explain the presence of the understory species in different natural communities, favoring more the neutral theory (Hubbell 2001) than stabilizing mechanisms (Chesson 2000). However, it is clear that both processes can simultaneously influence an understory species (Adler et al. 2007) and influence the dynamics of competition and coexistence in different plant neighborhoods.

On the other hand, because STAR and whole-plant carbon gain are variables that depend on multiple plant attributes and environmental factors, we propose that changes in these features must be used as a whole-plant trait-based approach to detect the environmental filtering of species within and among communities. In many cases, trait-based studies with a single variable have focused mainly to detect the coexistence (Adler et al. 2013), community assembly (Ackerly and Cornwell 2007), habitat filtering (Cornwell et al. 2006) and niches (Sterck et al. 2011) through features that do not necessarily reflect the complexity of the whole-plant adaptation to spatial and temporal variations. Plant indexes that consider the multidimensional response of plant adaptation due to temporal and spatial gradients of neighborhoods must be used as key factors to detect complex ecological dynamics in ecosystems, after costly intensive work.

In conclusion, we found that the local adaptation of plant architecture, leaf attributes and gas exchange of *P. padifolia* and *P. elata* by neighborhood structure and light availability are associated with the convergence in plant performance of light capture efficiency and net daily carbon gain. The above can be achieved by two pathways: (i) by changes in the plant architecture by distance-dependent neighborhood factors; or (ii) by changes in the carbon gain by light environments. Future work must be directed to demonstrate how whole-plant fitness parameters, e.g., light capture efficiency and carbon gain, are associated with stabilizing processes and fitness equality among communities as well as how this association allows for the survival and assembly of species.

Supplementary data

Supplementary data for this article are available at *Tree Physiology* Online.

Acknowledgments

Conflict of interest

None declared.

Funding

References

Ackerly DD, Cornwell WK (2007) A trait-based approach to community assembly: partitioning of species trait values into within- and among-community components. Ecol Lett 10:135–145.

Adler PB, HilleRisLambers J, Levine JM (2007) A niche for neutrality. Ecol Lett 10:95–104.

Adler PB, Fajardo A, Kleinhesselink AR, Kraft NJB (2013) Trait-based tests of coexistence mechanisms. Ecol Lett 16:1294–1306.

Allen MT, Pearcy RW (2000) Stomatal versus biochemical limitations to dynamic photosynthetic performance in four tropical rainforest shrub species. Oecologia 122:479–486.

Berger U, Piou C, Schiffers K, Grimm V (2008) Competition among plants: concepts, individual-based modelling approaches, and a proposal for a future research strategy. Perspect Plant Ecol Evol Syst 9:121–135.

Bittebiere A-K, Mony C, Clément B, Garbey M (2012) Modeling competition between plants using an individual based model: methods and effects on the growth of two species with contrasted growth forms. Ecol Modell 234:38–50.

Butterfield BJ, Callaway RM (2013) A functional comparative approach to facilitation and its context dependence. Funct Ecol 27:907–917.

Chazdon RL, Fetcher N (1984) Photosynthetic light environments in a lowland tropical rain forest in Costa Rica. J Ecol 72:553–564.

Chazdon RL, Pearcy RW (1991) The importance of sunflecks for forest understory plants. Bioscience 41:760–766.

Chesson P (2000) Mechanisms of maintenance of species diversity. Annu Rev Ecol Syst 31:343–366.

Cornwell WK, Ackerly DD (2009) Community assembly and shifts in plant trait distributions across an environmental gradient in coastal California. Ecol Monogr 79:109–126.

Cornwell WK, Schwilk DW, Ackerly DD (2006) A trait-based test for habitat filtering: convex hull volume. Ecology 87:1465–1471.

Craine JM, Dybzinski R (2013) Mechanisms of plant competition for nutrients, water and light. Funct Ecol 27:833–840.

Delagrange S, Montpied P, Dreyer E, Messier C, Sinoquet H (2006) Does shade improve light interception efficiency? A comparison among seedlings from shade-tolerant and -intolerant temperate deciduous tree species. New Phytol 172:293–304.

Duursma R, Cieslak M (2013) YplantQMC: plant architectural analysis with Yplant and QuasiMC. http://cran.r-project.org/web/packages/YplantQMC/ (3 August 2015, date last accessed).

Duursma RA, Falster DS, Valladares F et al. (2012) Light interception efficiency explained by two simple variables: a test using a diversity of small- to medium-sized woody plants. New Phytol 193:397–408.

Ethier GJ, Livingston NJ (2004) On the need to incorporate sensitivity to CO_2 transfer conductance into the Farquhar–von Caemmerer–Berry leaf photosynthesis model. Plant Cell Environ 27:137–153.

Evans J, Poorter H (2001) Photosynthetic acclimation of plants to growth irradiance: the relative importance of specific leaf area and nitrogen partitioning in maximizing carbon gain. Plant Cell Environ 24:755–767.

Falster DS, Westoby M (2003) Plant height and evolutionary games. Trends Ecol Evol 18:337–343.

Farquhar GD, von Caemmerer SV, Berry JA (1980) A biochemical model of photosynthetic CO_2 assimilation in leaves of C_3 species. Planta 149:78–90.

Finegan B (1996) Pattern and process in neotropical secondary rain forests: the first 100 years of succession. Trends Ecol Evol 11:119–124.

Freckleton RP, Watkinson AR (1999) The mis-measurement of plant competition. Funct Ecol 13:285–287.

Gálvez D, Pearcy RW (2003) Petiole twisting in the crowns of *Psychotria limonesis*: implications for light interception and daily carbon gain. Oecologia 135:22–29.

Goldberg DE (1987) Neighborhood competition in an old-field plant community. Ecology 68:1211–1223.

Grime JP (1979) Plant strategies and vegetation processes. John Wiley & Sons, Chichester, England, pp 1–403.

Grote S, Condit R, Hubbell S, Wirth C, Rüger N (2013) Response of demographic rates of tropical trees to light availability: can position-based competition indices replace information from canopy census data? PLoS One 8:e81787. doi:10.1371/journal.pone.0081787

Grothendieck G (2014) nls2: non-linear regression with brute force. http://cran.r-project.org/web/packages/nls2/ (3 August 2015, date last accessed).

Guzmán J (2015) Analisis ecomorfofisiológico de la competencia de vecindarios boscosos sobre dos arbustos del sotobosque en un bosque nuboso. Master thesis, Universidad de Costa Rica, Costa Rica.

Hallé F, Oldeman RAA, Tomlinson PB (1978) Tropical trees and forests: an architectural analysis. Springer, Berlin, Germany, pp 1–386.

Hubbell SP (2001) The unified neutral theory of biodiversity and biogeography. Princeton University Press, Princeton, NJ, USA, pp 1–370.

Hubbell SP, Foster RB, O'Brien ST, Harms KE, Condit R, Wechsler B, Wright S, De Lao SL (1999) Light-gap disturbances, recruitment limitation, and tree diversity in a neotropical forest. Science 283:554–557.

Huston M, Smith T (1987) Plant succession: life history and competition. Am Nat 130:168–198.

ITCR (2008) Atlas digital de Costa Rica. Laboratorio de Sistemas de Información Geográfica, Escuela de Ingeniería Forestal, Instituto Tecnológico de Costa Rica, Cartago, Costa Rica.

Kabakoff RP, Chazdon RL (1996) Effects of canopy species dominance on understorey light availability in low-elevation secondary forest stands in Costa Rica. J Trop Ecol 12:779–788.

Kitajima K, Mulkey SS, Wright SJ (2005) Variation in crown light utilization characteristics among tropical canopy trees. Ann Bot 95:535–547.

Kuiper P (1961) The effects of environmental factors on the transpiration of leaves, with special reference to stomatal light response. Meded Landbouwhoogeschool (Wageningen) 61:1–49.

Lusk CH, Pérez-Millaqueo MM, Piper FI, Saldaña A (2011) Ontogeny, understorey light interception and simulated carbon gain of juvenile rainforest evergreens differing in shade tolerance. Ann Bot 108:419–428.

Marshall B, Biscoe PV (1980) A model for C_3 leaves describing the dependence of net photosynthesis on irradiance. J Exp Bot 31:29–39.

Medrano H, Escalona JM, Bota J, Gulías J, Flexas J (2002) Regulation of photosynthesis of C_3 plants in response to progressive drought: stomatal conductance as a reference parameter. Ann Bot 89:895–905.

Niinemets Ü, Kull O, Tenhunen JD (1998) An analysis of light effects on foliar morphology, physiology, and light interception in temperate deciduous woody species of contrasting shade tolerance. Tree Physiol 18:681–696.

Pearcy RW (1987) Photosynthetic gas exchange responses of Australian tropical forest trees in canopy, gap and understory micro-environments. Funct Ecol 1:169–178.

Pearcy RW, Yang W (1996) A three-dimensional crown architecture model for assessment of light capture and carbon gain by understory plants. Oecologia 108:1–12.

Pearcy RW, Valladares F, Wright SJ, De Paulis EL (2004) A functional analysis of the crown architecture of tropical forest *Psychotria* species: do species vary in light capture efficiency and consequently in carbon gain and growth? Oecologia 139:163–177.

Pearcy RW, Muraoka H, Valladares F (2005) Crown architecture in sun and shade environments: assessing function and trade-offs with a three-dimensional simulation model. New Phytol 166:791–800.

Pearcy RW, Duursma RA, Falster DS (2013) Studying plant architecture with Y-plant and 3D digitising. http://prometheuswiki.publish.csiro.au/tiki-index.php?page=Studying+plant+architecture+with+Y-plant+and+3D+digitising (3 August 2015, date last accessed).

Pérez-Harguindeguy N, Díaz S, Garnier E et al. (2013) New handbook for standardised measurement of plant functional traits worldwide. Aust J Bot 61:167–234.

Pérez-Molina JP, Cordero RA (2012) Recuperación de tres coberturas forestales de altura media en Costa Rica: análisis de los oligoquetos, el mantillo y suelo. Rev Biol Trop 60:1431–1443.

Quinn GP, Keough MJ (2002) Experimental design and data analysis for biologists. Cambridge University Press, New York, USA, pp 425–442.

R Development Core Team (2014) R: a language and environment for statistical computing. http://www.r-project.org (3 August 2015, date last accessed).

Reich PB, Wright IJ, Cavender-Bares J, Craine JM, Oleksyn J, Westoby M, Walters MB (2003) The evolution of plant functional variation: traits, spectra, and strategies. Int J Plant Sci 164:S143–S164.

Rich P (1989) A manual for analysis of hemispherical canopy photography. Los Alamos National Laboratory Report, NM, USA, pp 1–80.

Ringle CM, Wende S, Becker J-M (2014) SmartPLS 3. www.smartpls.com (3 August 2015, date last accessed).

Schwinning S, Weiner J (1998) Mechanisms determining the degree of size asymmetry in competition among plants. Oecologia 113:447–455.

Shipley B, Lechowicz MJ, Wright I, Reich PB (2006) Fundamental trade-offs generating the worldwide leaf economics spectrum. Ecology 87:535–541.

Sterck F, Markesteijn L, Schieving F, Poorter L (2011) Functional traits determine trade-offs and niches in a tropical forest community. Proc Natl Acad Sci USA 108:20627–20632.

Sterck FJ, Duursma RA, Pearcy RW, Valladares F, Cieslak M, Weemstra M (2013) Plasticity influencing the light compensation point offsets the specialization for light niches across shrub species in a tropical forest understorey. J Ecol 101:971–980.

Takenaka A (1994) Effects of leaf blade narrowness and petiole length on the light capture efficiency of a shoot. Ecol Res 9:109–114.

Tambussi EA, Graciano C (2010) Técnicas de medición de intercambio de gases en plantas: curvas de respuesta a la luz y al CO_2. In: Fernández ME, Gyenge JE (eds) Técnicas de medición en ecofisiología vegetal: conceptos y procedimientos. Ediciones INTA, Buenos Aires, Argentina, pp 109–115.

Taylor CM (1989) Revision of Palicourea (Rubiaceae) in Mexico and Central America. Syst Bot Monogr 26:1–102.

Thornley JH, Johnson IR (1990) Plant and crop modelling: a mathematical approach to plant and crop physiology. The Blackbur Press, New Jersey, USA, pp 243–263.

Tremmel DC, Bazzaz FA (1995) Plant architecture and allocation in different neighborhoods: implications for competitive success. Ecology 76:262–271.

Trinder CJ, Brooker RW, Davidson H, Robinson D (2012) A new hammer to crack an old nut: interspecific competitive resource capture by plants is regulated by nutrient supply, not climate. PLoS One 7:e29413. doi:10.1371/journal.pone.0029413

Trinder CJ, Brooker RW, Robinson D (2013) Plant ecology's guilty little secret: understanding the dynamics of plant competition. Funct Ecol 27:918–929.

Valladares F, Niinemets Ü (2008) Shade tolerance, a key plant feature of complex nature and consequences. Annu Rev Ecol Evol Syst 39:237–257.

Valladares F, Skillman JB, Pearcy RW (2002) Convergence in light capture efficiencies among tropical forest understory plants with contrasting crown architectures: a case of morphological compensation. Am J Bot 89:1275–1284.

Weigelt A, Jolliffe P (2003) Indices of plant competition. J Ecol 91:707–720.

Weiner J (1984) Neighbourhood interference amongst *Pinus rigida* individuals. J Ecol 72:183–195.

Wright IJ, Reich PB, Cornelissen JHC et al. (2005) Assessing the generality of global leaf trait relationships. New Phytol 166:485–496.

Zar J (2010) Biostatistical analysis, 5th edn. Prentice-Hall Inc., Upper Saddle River, New Jersey, USA, pp 605–624.